Electronic Supplementary Material (ESI) for Materials Chemistry Frontiers.

Electronic Supplementary Information

Metal-Organic-Framework Embellished through Ion Etching Method for Highly Enhanced Electrochemical Oxygen Evolution

Qiuxiang Mou,[a] Zhenhang Xu,[b] Wei Zuo,[b] Tianyu Shi,[b] Erlei Li,[a] Gongzhen Cheng,[b] Xinghai Liu,[a] Huaming Zheng,[*c] Houbin Li,[*a] and Pingping Zhao[*a]

[a] *Research Center of Graphic Communication, Printing and Packaging, Wuhan University, Wuhan, 430072, China.*
[b] *College of Chemistry and Molecular Sciences, Wuhan University, Wuhan, 430072, China.*
[c] *School of Material Sciences & Engineering, Wuhan Institute of Technology, Wuhan, 430073 Hubei, P.R. China.*

Table of contents

1. Supplementary Figures

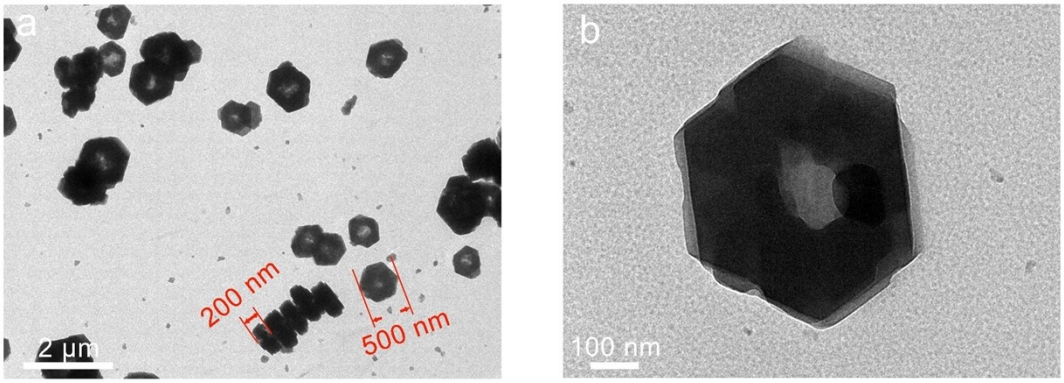

Fig. S1. TEM images of Ni MOF.

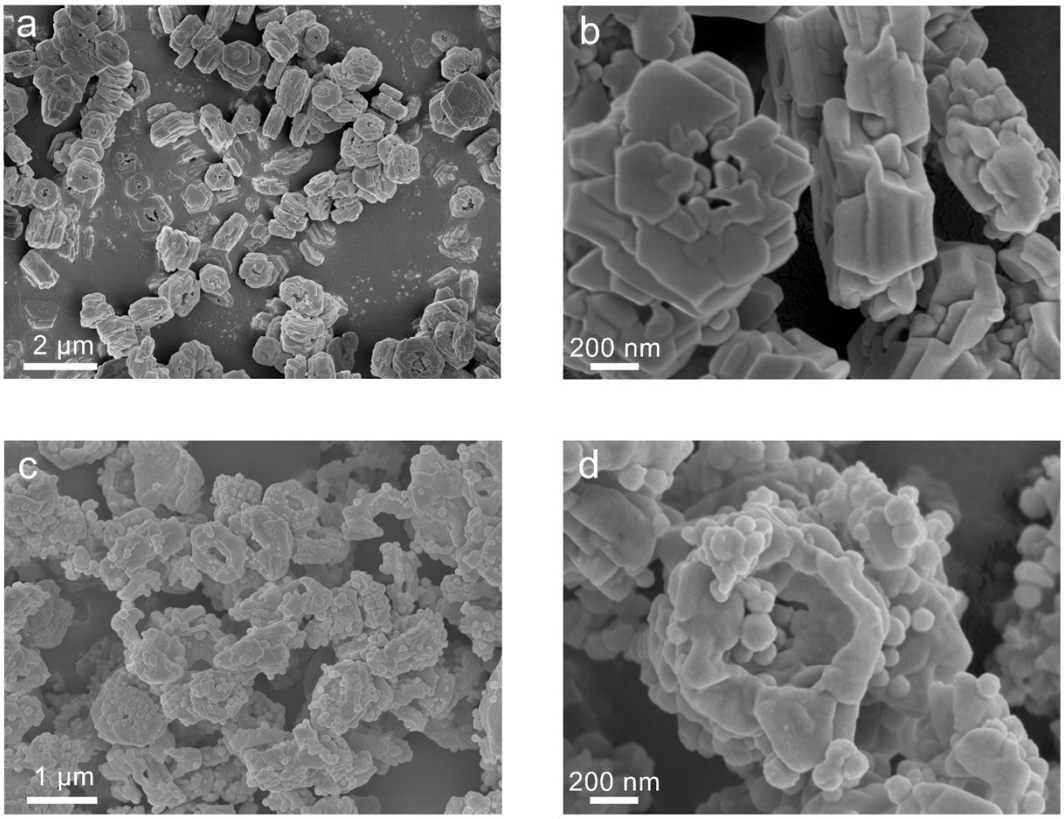

Fig. S2. SEM images of (a) (b)Ni MOF and (c) (d) Ni-MOF-Fe-2.

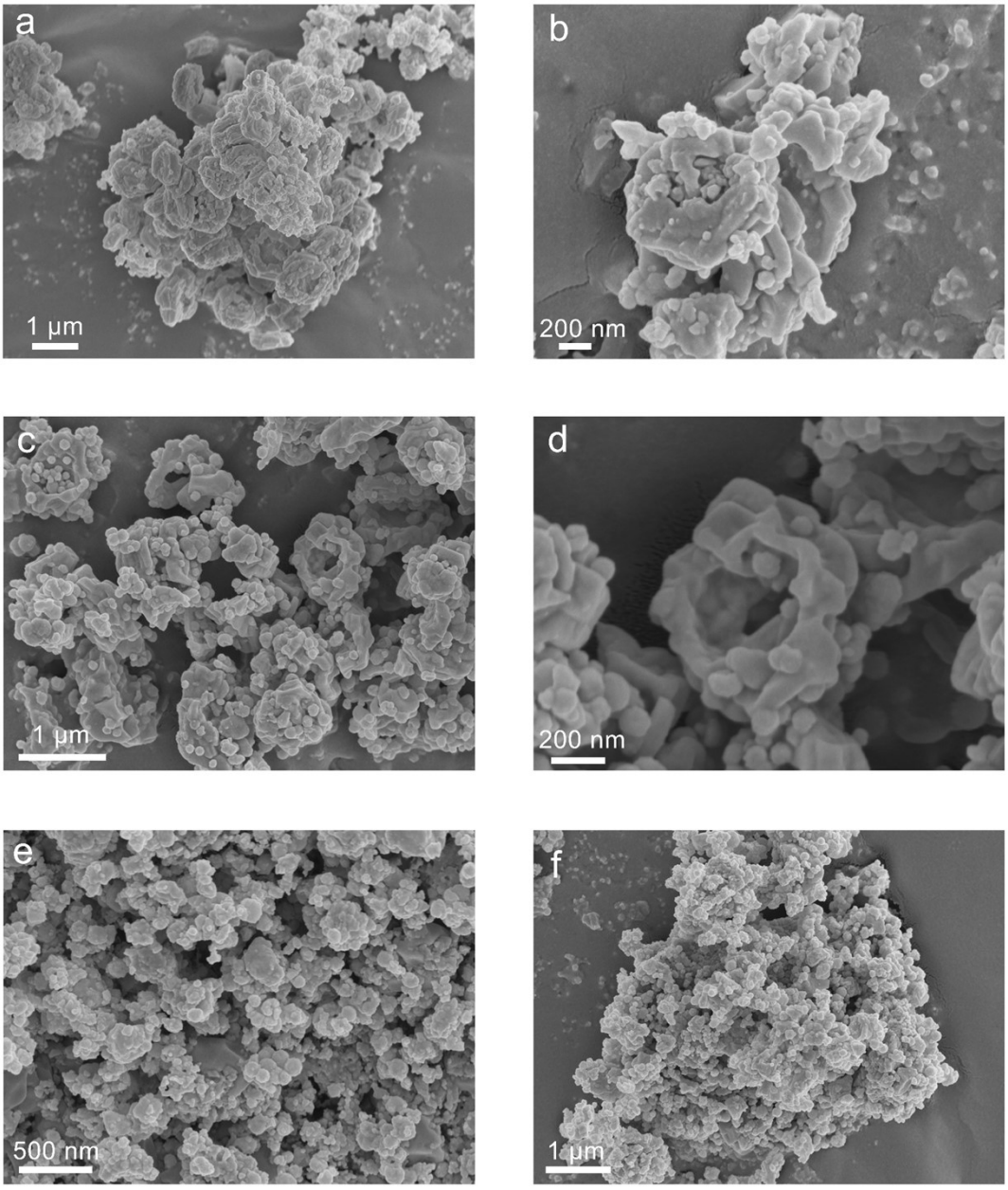

Fig. S3. SEM images of (a) (b) Ni-MOF-Fe-1, (c) (d) Ni-MOF-Fe-2 and (e) (f) Ni-MOF-Fe-3.

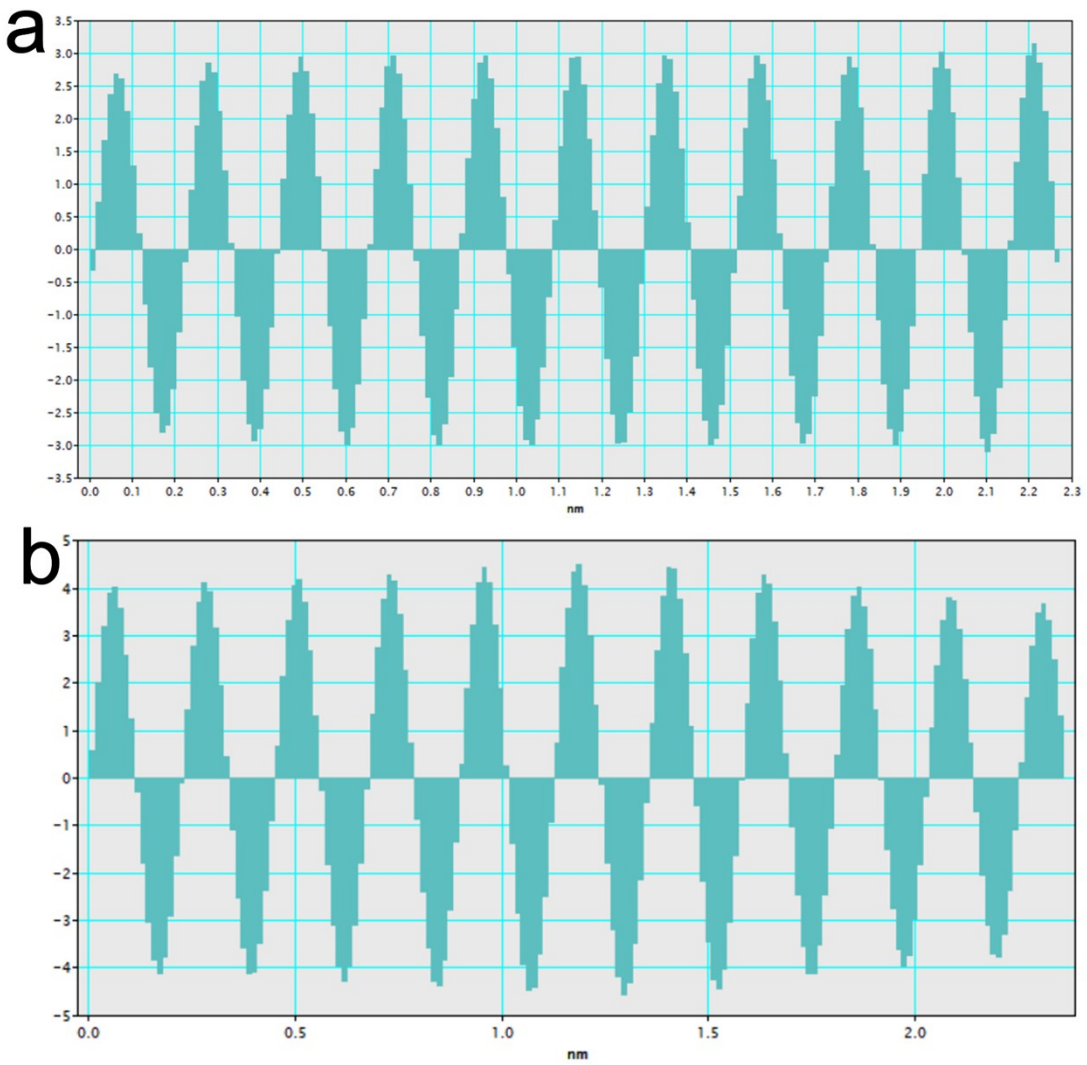

Fig. S4. Contrast intensity profile of the (a) (-121) plane and (b) (-120) plane.

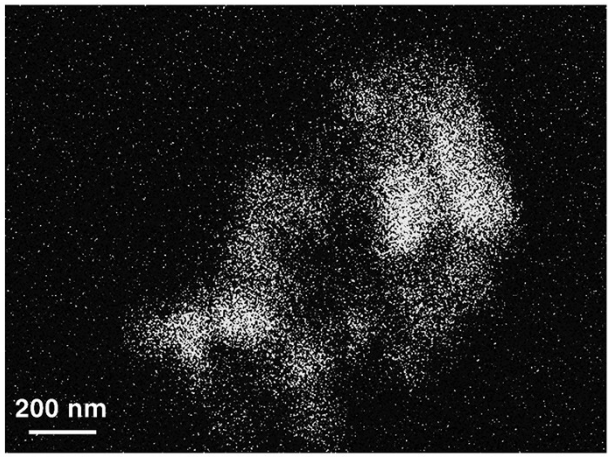

Fig. S5. HAADF-STEM image of Ni-MOF-Fe-2.

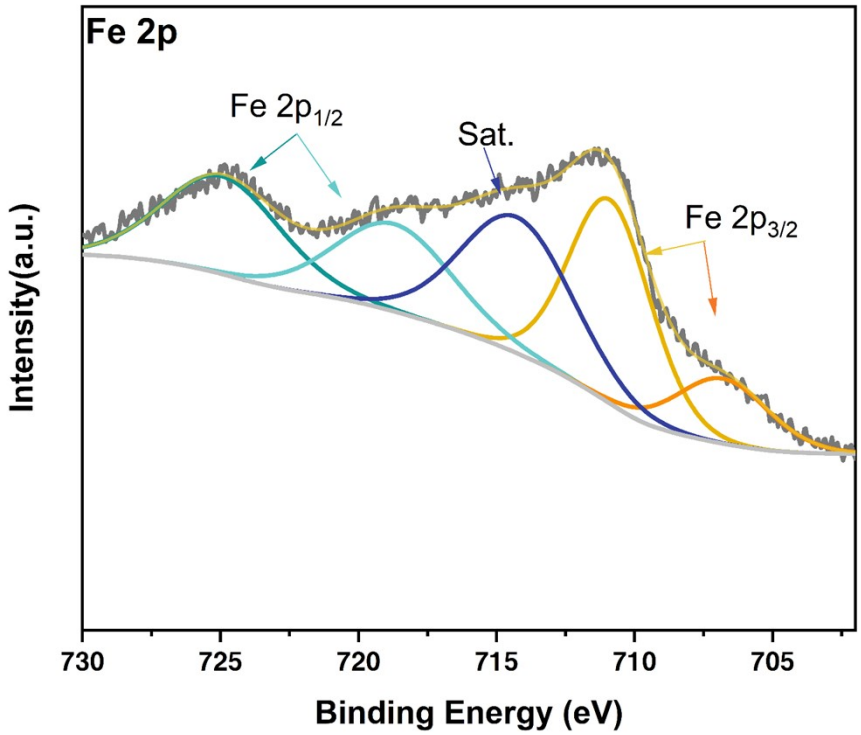

Fig. S6. High-resolution XPS spectrum of Fe 2p in Ni-MOF-Fe-2.

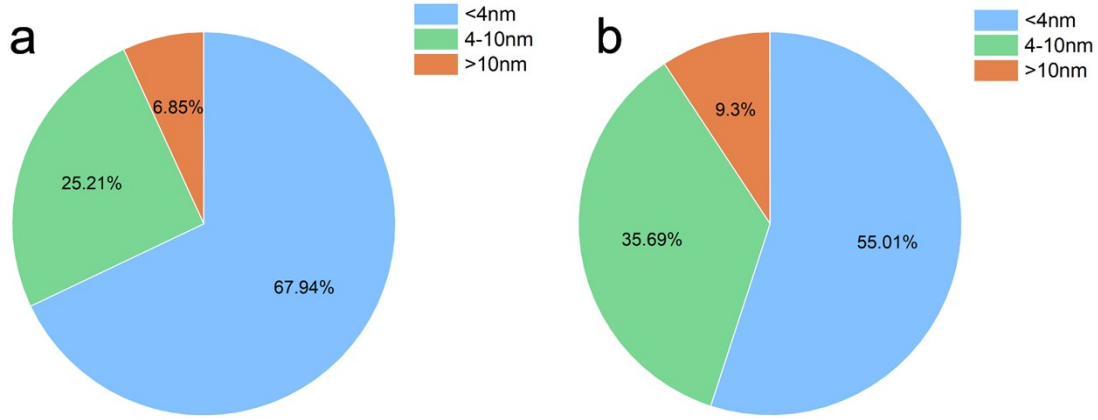

Fig. S7. Pie charts of pore width in (a) Ni MOF and (b) Ni-MOF-Fe-2, where the pore width proportion of Ni-MOF-Fe-2 showed a wider distribution than that of Ni MOF, and more big pores generated in Ni-MOF-Fe-2, intuitively indicating that the structure of MOF etched by iron ions has been effectively changed.

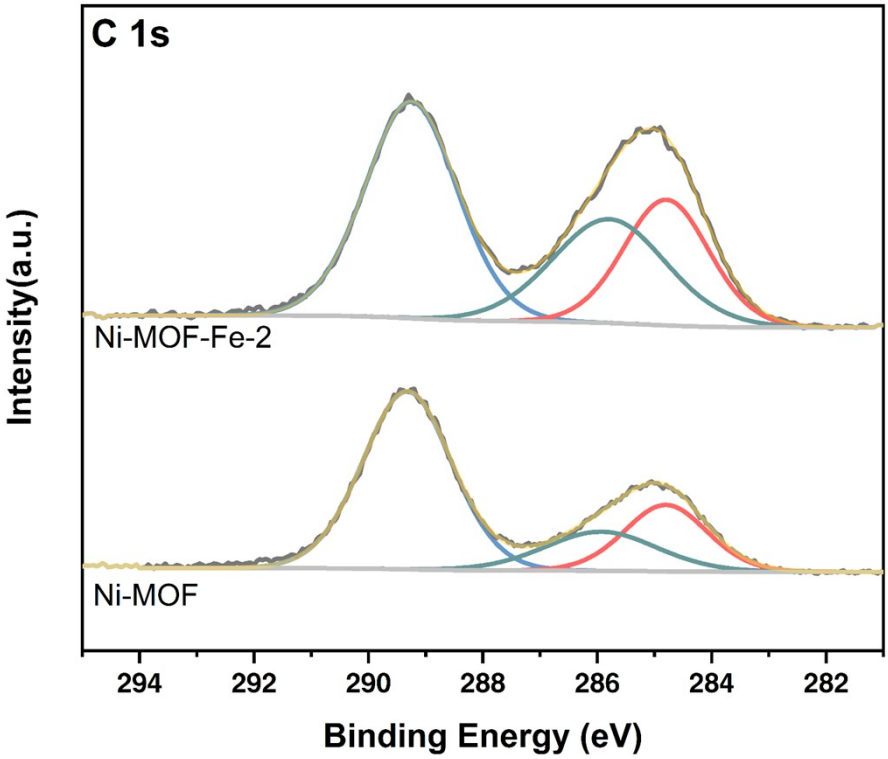

Fig. S8. High-resolution XPS spectra of C 1s in Ni MOF and Ni-MOF-Fe-2.

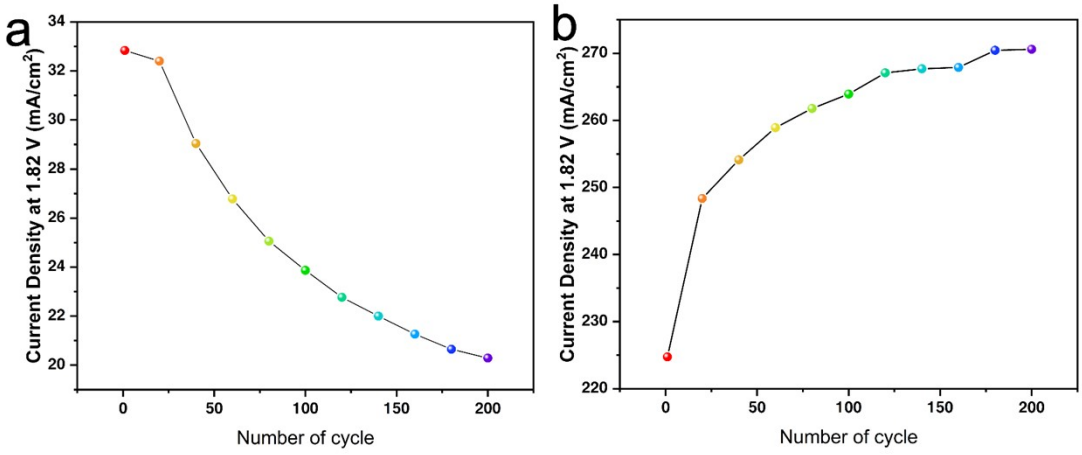

Fig. S9. OER activity at 1.66 V (vs. RHE) for (a) Ni MOF and (b) Ni-MOF-Fe-2.

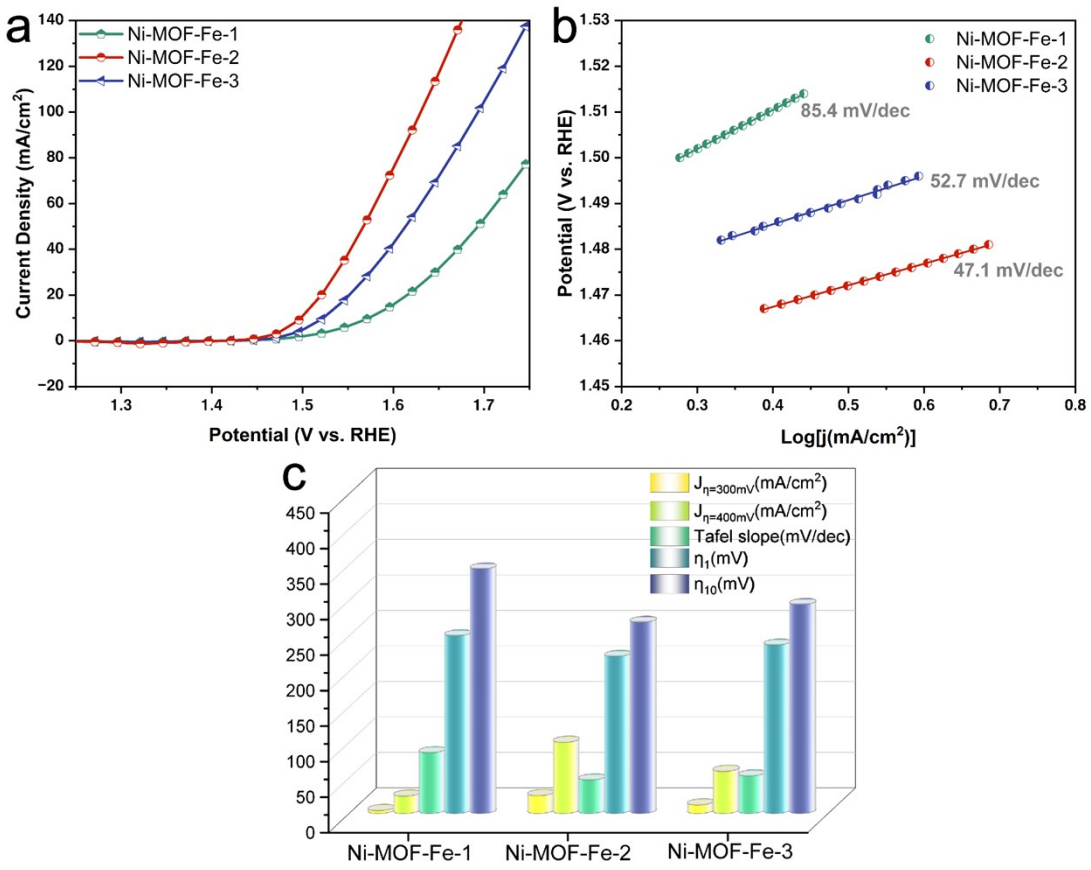

Fig. S10. OER activity of the Fe etching catalysts. (a) LSV OER polarization curves of the catalysts without *i*R-correction. (b) Corresponding Tafel slopes in (a). (c) Comparison of the overpotentials at 1 mA/cm^2 (η_1) and 10 mA/cm^2 (η_{10}), the current densities under an overpotential of 300 mV and 400 mV, and the Tafel slopes obtained from the catalysts.

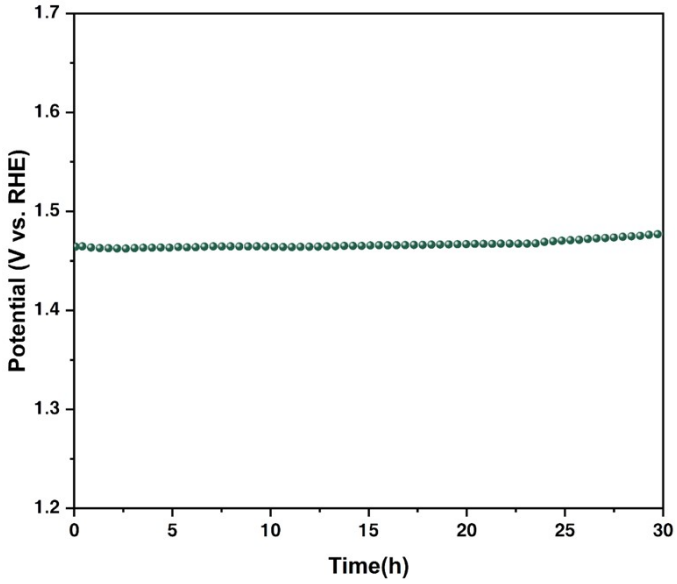

Fig. S11. Chronopotentiometric curve of Ni-MOF-Fe-2 at 10 mA/cm^2.

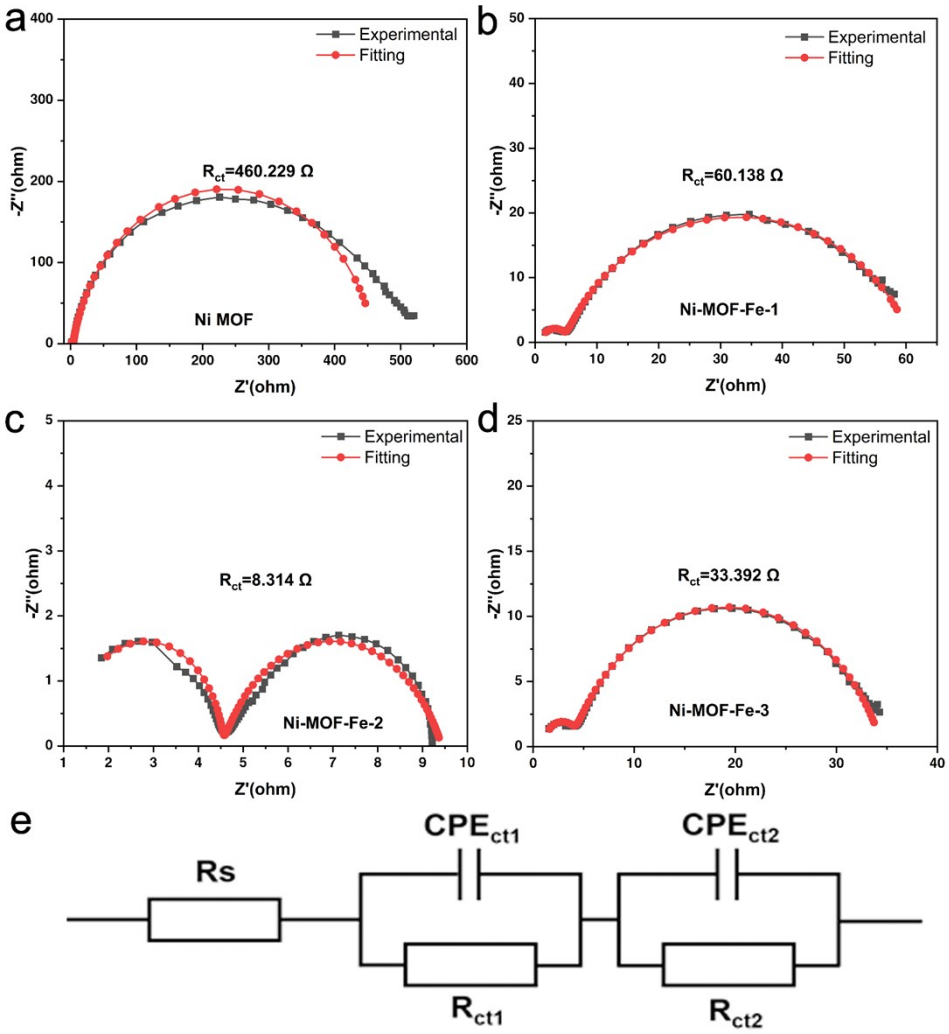

Fig. S12. Expereimental data and fitting results of (a) Ni MOF, (b) Ni-MOF-Fe-1, (c) Ni-MOF-Fe-2 and (d) Ni-MOF-Fe-3. (e) The equivalent circuit for modeling the measured electrochemical response in this manuscript.

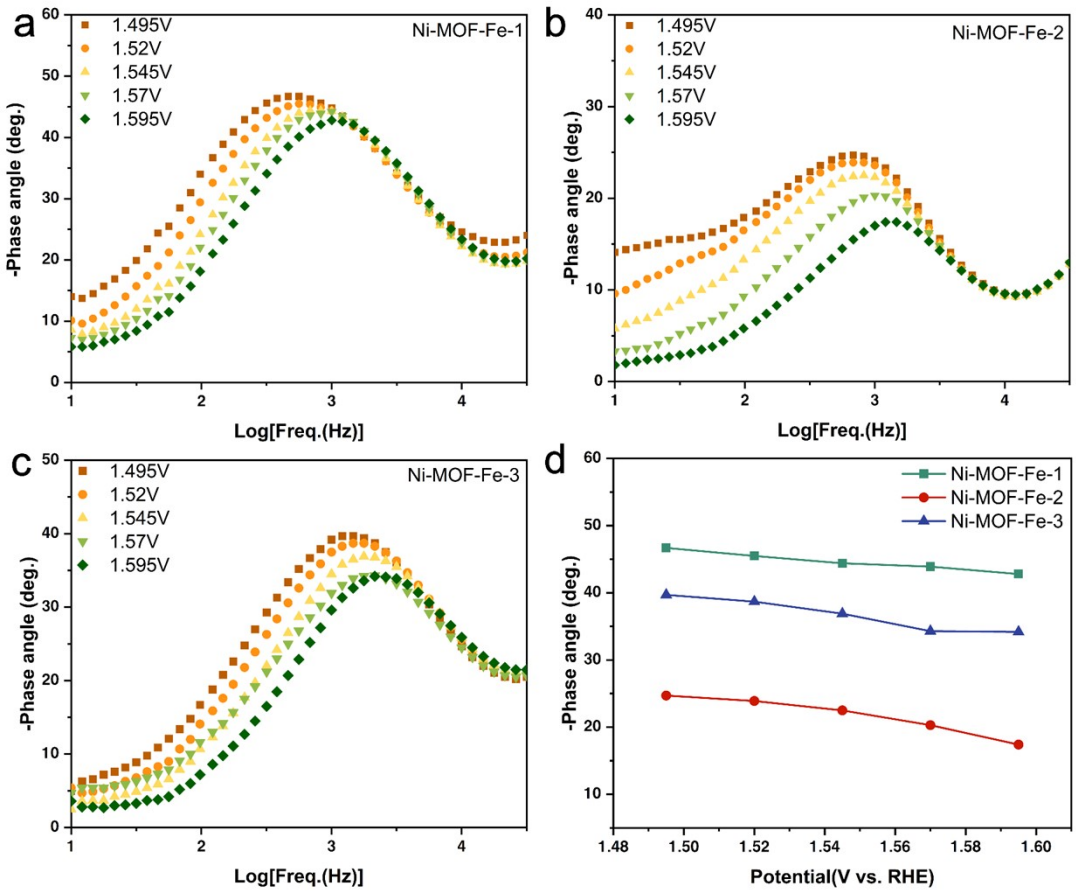

Fig. S13. Bode plots of (a) Ni-MOF-Fe-1, (b) Ni-MOF-Fe-2 and (c) Ni-MOF-Fe-3 obtained under different potentials. (d) Potential dependence of the phase angle of the samples.

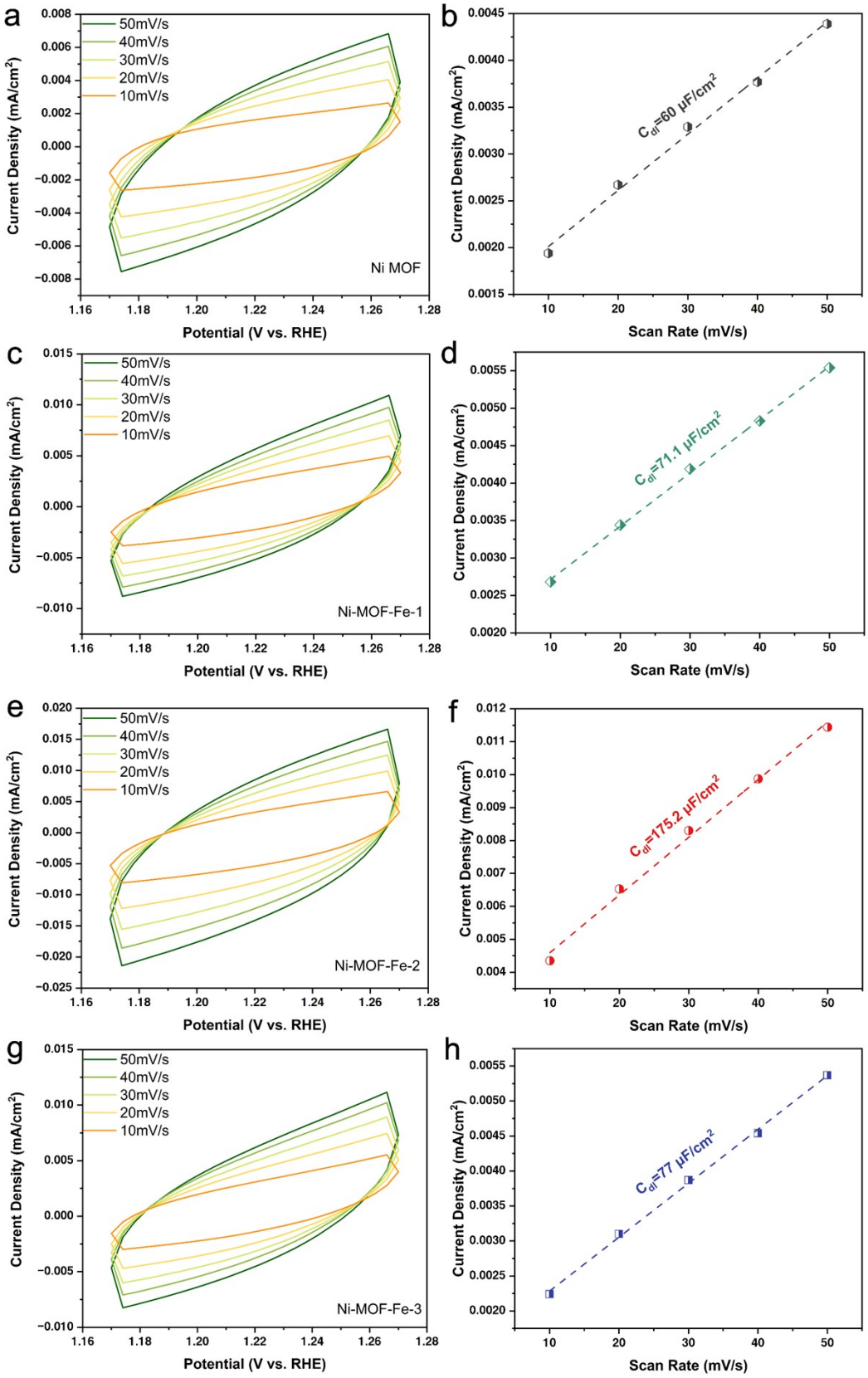

Fig. S14. CV curves and current density differences at 1.222 V vs. RHE against the scan rate for the estimation of C_{dl} of the samples. (a) (b) Ni MOF, (c) (d) Ni-MOF-Fe-1, (e) (f) Ni-MOF-Fe-2. (g) (h) Ni-MOF-Fe-3.

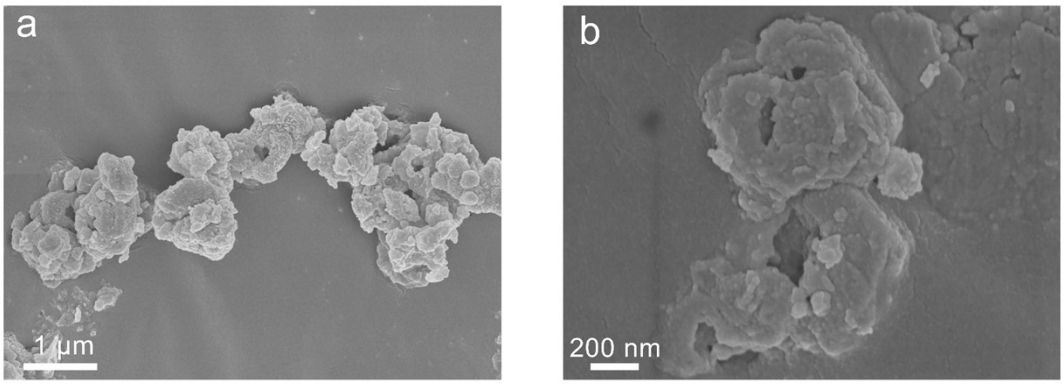

Fig. S15. SEM images of the post-OER Ni-MOF-Fe-2.

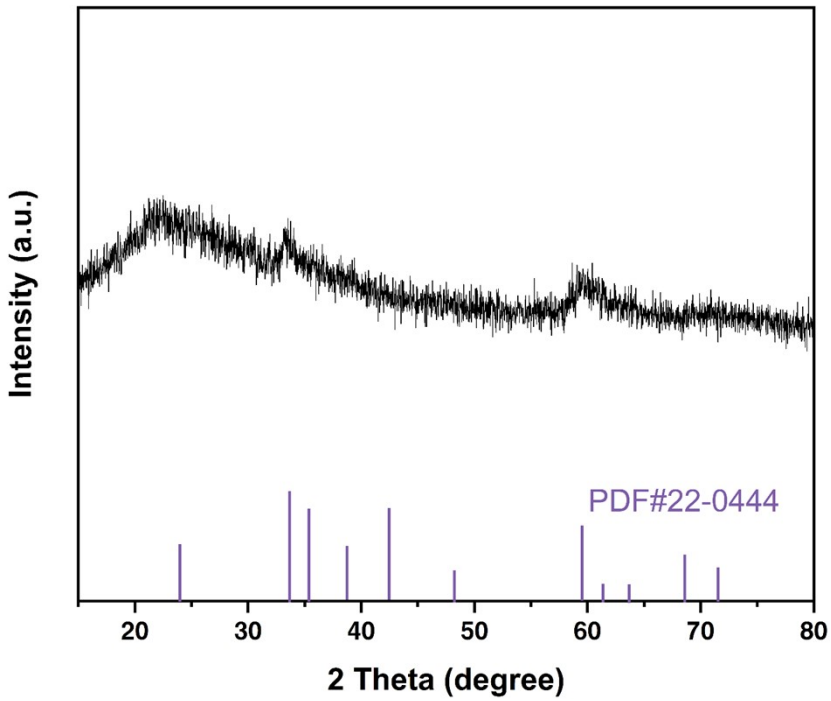

Fig. S16. XRD pattern of the post-OER Ni-MOF-Fe-2.

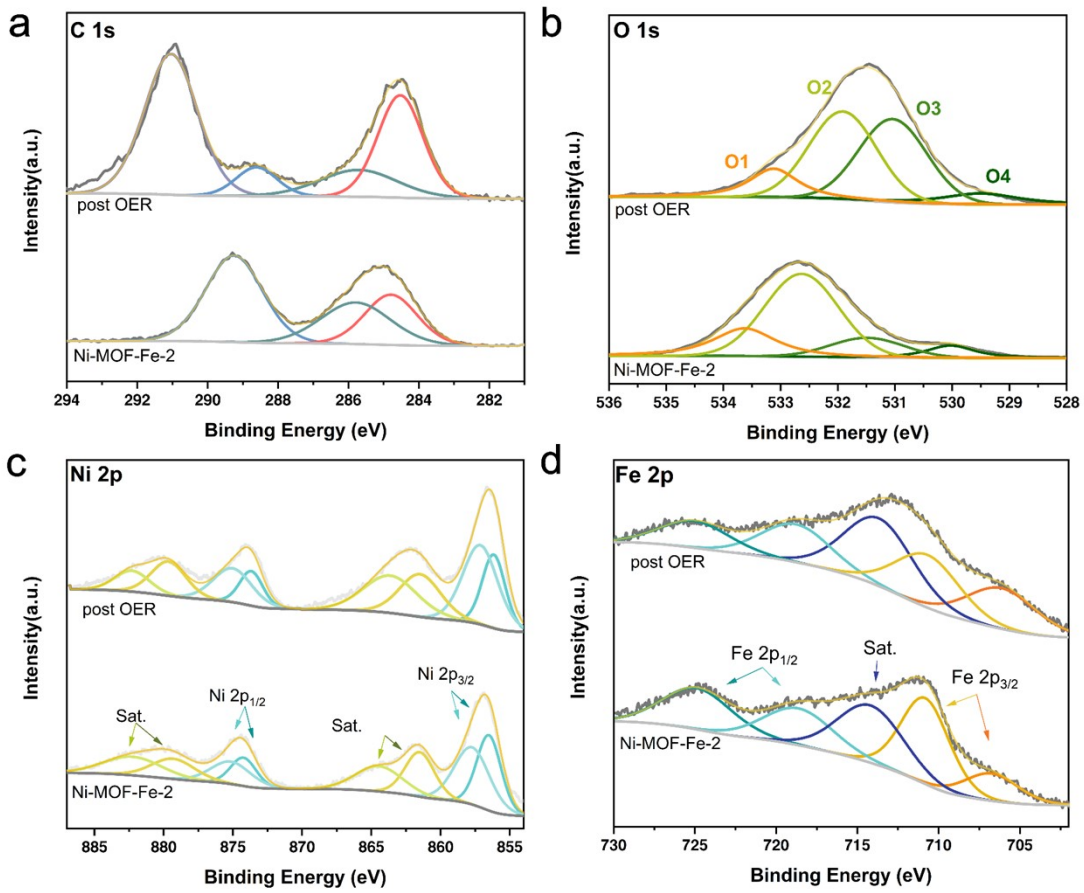

Fig. S17. High-resolution XPS spectra of (a) C 1s, (b) O 1s (c) Ni 2p and (d) Fe 2p of Ni-MOF-Fe-2 before and after OER process.

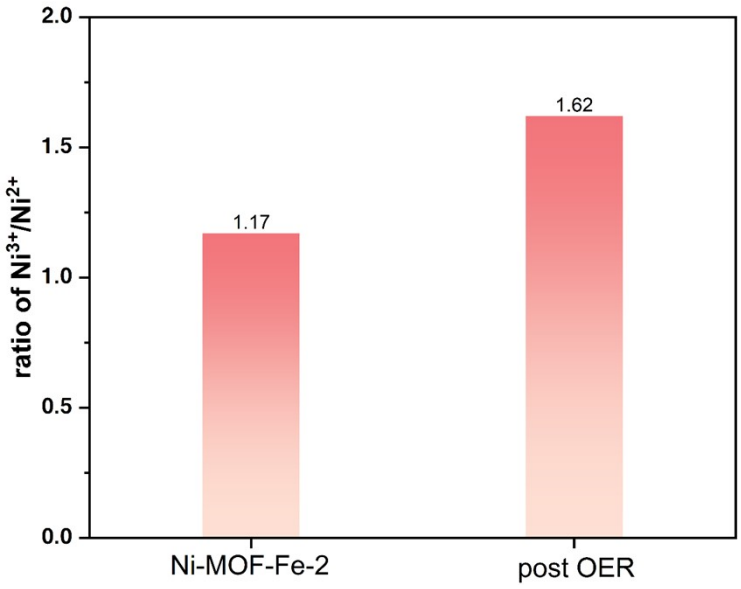

Fig. S18. Ratio of Ni^{3+}/Ni^{2+} in Ni-MOF-Fe-2 before and after OER process.

2. Supplementary Tables

Table S1. EDX results of Ni-MOF-Fe-2.

Element	Weight(%)	Atomic(%)	Net Error(%)
O K	37.01	67.82	0.94
Fe K	28.46	14.94	1.05
Ni K	34.53	17.24	0.17

Table S2. Comparison of OER performance of catalysts in this work with reported electrocatalysts.

Catalyst	η(mV) at 10 mA cm^{-2}	Tafel Slope (mV dec^{-1})	Electrolyte	Loading mass (μg cm^{-2})	Reference
Ni-MOF-Fe-2	269	47.1	1 M KOH	300	
Ni-MOF-Fe-1	344	85.4	1 M KOH	300	This work
Ni-MOF-Fe-3	294	52.7	1 M KOH	300	
Ni SAs@S/N-CMF	285	50.8	1 M KOH	750	[1]
BCN/ZrO_2	301	75	1 M KOH	141	[2]
Ru@NiV-LDH	272	60	1 M KOH	100	[3]
FeNi/$(FeNi)_9S_8$/N	283	64.03	1 M KOH	420	[4]
CoFe-LDH/GP	252	61	1 M KOH	6500	[5]
3Co-LaMOH|O_V@NC	330	129	0.1 M KOH	500	[6]
CoNi-SAs/NC	340	58.7	1 M KOH	1400	[7]
CO-Fe_2O_3	439	99	0.1 M KOH	784	[8]
NCMC	290	73	1 M KOH	280	[9]
Co/MoC@N-C	290	90	1 M KOH	455	[10]
Ni_3S_2	295	52	1 M KOH	600	[11]
NiFeZr MOFs-0.12	288	66	1 M KOH	250	[12]
CoP NFs	323	49.6	1 M KOH	265	[13]
Ni-MOF@CNT	370	138.2	1 M KOH	1000	[14]
CoP/NCNHP	310	70	1 M KOH	400	[15]
NiCu-MOF	290	169	1 M KOH	2000	[16]
Co_3S_4@MoS_2	280	43	1 M KOH	283	[17]
NiFe-HXR	289	43	1 M KOH	150	[18]
Fe_2/Co_1 GNCL	350	70	1 M KOH	255	[19]
NiFe MOF|OM NFH	270	123	1 M KOH	400	[20]
W_2N/WC	320	94.5	1 M KOH	200	[21]
Mo-Co_3O_4/CNTs	280	63	1 M KOH	250	[22]
CoFeBiP	273	77.3	1 M KOH	300	[23]
VC-MOF-Fe	339	78	1 M KOH	500	[24]
NiPc-$NiFe_{0.09}$	300	55	1 M KOH	285	[25]
Fe-Co_3O_4	262	43	1 M KOH	250	[26]

ZIF-9(III)/Co LDH-15	297	65	1 M KOH	189	[27]
Co_2P/CoNPC	326	72.6	1 M KOH	390	[28]
MOF3_A	424	--	0.5 M KOH	125	[29]
Co_2FeO_4/NCNTs	420	96.7	0.1 M KOH	200	[30]
aMOF-NC	249	39.5	1 M KOH	250	[31]
$Co_{1.5}Fe_{0.5}P$	278	57	1 M KOH	250	[32]
FeCo(OH)x-30	295	59	1 M KOH	255	[33]
O-CoMoS	272	45	1 M KOH	1000	[34]
(Co,0.3Ni-HMT)	330	66	1 M KOH	182	[35]

Table S3. EIS parameters of the catalysts.

catalysts	R_s (Ω)	R_{ct1} (Ω)	CPE_{ct1} (mF)	R_{ct2} (Ω)	CPE_{ct2} (mF)	R_{ct} (Ω)
Ni MOF	1.237	2.829	1.119	457.4	0.88477	460.23
Ni-MOF-Fe-1	0.95117	3.748	0.98628	56.39	0.76604	60.14
Ni-MOF-Fe-2	1.111	3.436	0.95588	4.878	0.74285	8.31
Ni-MOF-Fe-3	1.166	2.612	1.097	30.84	0.77259	33.39

Note: R_{ct} is equal to R_{ct1} plus to R_{ct2}.

3. Reference

[1]Zhao, Y.; Guo, Y.; Lu, X. F.; Luan, D.; Gu, X.; Lou, X. W. D., Exposing Single-Ni Atoms in Hollow S/N-doped Carbon Macroporous Fibers for Highly Efficient Electrochemical Oxygen Evolution. *Adv Mater* **2022**, e2203442.

[2]Ahsan, M. A.; He, T.; Eid, K.; Abdullah, A. M.; Sanad, M. F.; Aldalbahi, A.; Alvarado-Tenorio, B.; Du, A.; Puente Santiago, A. R.; Noveron, J. C., Controlling the Interfacial Charge Polarization of MOF-Derived 0D-2D vdW Architectures as a Unique Strategy for Bifunctional Oxygen Electrocatalysis. *ACS Appl Mater Interfaces* **2022,** *14* (3), 3919-3929.

[3]Karmakar, A.; Karthick, K.; Sankar, S. S.; Kumaravel, S.; Madhu, R.; Bera, K.; Dhandapani, H. N.; Nagappan, S.; Murugan, P.; Kundu, S., Stabilization of ruthenium nanoparticles over NiV-LDH surface for enhanced electrochemical water splitting: an oxygen vacancy approach. *Journal of Materials Chemistry A* **2022,** *10* (7), 3618-3632.

[4]Meng, H. L.; Lin, S. Y.; Feng, J. J.; Zhang, L.; Wang, A. J., Coordination regulated pyrolysis synthesis of ultrafine FeNi/$(FeNi)_9S_8$ nanoclusters/nitrogen, sulfur-codoped graphitic carbon nanosheets as efficient bifunctional oxygen electrocatalysts. *Journal of Colloid and Interface Science* **2022,** *610*, 573-582.

[5]Deng, B.; Liang, J.; Yue, L. C.; Li, T. S.; Liu, Q.; Liu, Y.; Gao, S. Y.; Alshehri, A. A.; Alzahrani, K. A.; Luo, Y. L.; Sun, X. P., CoFe-LDH nanowire arrays on graphite felt: A high-performance oxygen evolution electrocatalyst in alkaline media. *Chinese Chemical Letters* **2022,** *33* (2), 890-892.

[6]Zhang, J.; Chen, J.; Luo, Y.; Chen, Y.; Zhang, C.; Luo, Y.; Xue, Y.; Liu, H.; Wang, G.; Wang, R., Engineering heterointerfaces coupled with oxygen vacancies in lanthanum–based hollow microspheres for synergistically enhanced oxygen electrocatalysis. *Journal of Energy Chemistry* **2021,** *60*, 503-511.

[7]Han, X.; Ling, X.; Yu, D.; Xie, D.; Li, L.; Peng, S.; Zhong, C.; Zhao, N.; Deng, Y.; Hu, W., Atomically Dispersed Binary Co-Ni Sites in Nitrogen-Doped Hollow Carbon Nanocubes for Reversible Oxygen Reduction and Evolution. *Advanced Materials* **2019,** *31* (49), e1905622.

[8]Niu, Y.; Yuan, Y.; Zhang, Q.; Chang, F.; Yang, L.; Chen, Z.; Bai, Z., Morphology-controlled synthesis of metal-organic frameworks derived lattice plane-altered iron oxide for efficient trifunctional electrocatalysts. *Nano Energy* **2021,** *82*, 105699.

[9]Wei, X.; Zhang, Y.; He, H.; Gao, D.; Hu, J.; Peng, H.; Peng, L.; Xiao, S.; Xiao, P., Carbon-incorporated NiO/Co_3O_4 concave surface microcubes derived from a MOF precursor for overall water splitting. *Chemical Communications (Cambridge, England)* **2019,** *55* (46), 6515-6518.

[10]Huang, H.; Kong, L.; Liu, M.; He, J.; Shuang, W.; Xu, Y.; Bu, X.-H., Constructing bifunctional Co/MoC@N-C catalyst via an in-situ encapsulation strategy for efficient oxygen electrocatalysis. *Journal of Energy Chemistry* **2021,** *59*, 538-546.

[11]Zheng, X.; Han, X.; Zhang, Y.; Wang, J.; Zhong, C.; Deng, Y.; Hu, W., Controllable synthesis of nickel sulfide nanocatalysts and their phase-dependent performance for overall water splitting. *Nanoscale* **2019,** *11* (12), 5646-5654.

[12]Wang, Y.; Tang, W.; Li, X.; Wei, D., Improving the electrocatalytic activity of NiFe bimetal-organic framework toward oxygen evolution reaction by Zr doping. *Electrochimica Acta* **2021,** *381*, 138292.

[13]Ji, L.; Wang, J.; Teng, X.; Meyer, T. J.; Chen, Z., CoP Nanoframes as Bifunctional Electrocatalysts for Efficient Overall Water Splitting. *Acs Catalysis* **2019,** *10* (1), 412-419.
[14]Sreekanth, T. V. M.; Dillip, G. R.; Nagajyothi, P. C.; Yoo, K.; Kim, J., Integration of Marigold 3D flower-like Ni-MOF self-assembled on MWCNTs via microwave irradiation for high-performance electrocatalytic alcohol oxidation and oxygen evolution reactions. *Applied Catalysis B: Environmental* **2021,** *285*, 119793.
[15]Pan, Y.; Sun, K.; Liu, S.; Cao, X.; Wu, K.; Cheong, W. C.; Chen, Z.; Wang, Y.; Li, Y.; Liu, Y.; Wang, D.; Peng, Q.; Chen, C.; Li, Y., Core-Shell ZIF-8@ZIF-67-Derived CoP Nanoparticle-Embedded N-Doped Carbon Nanotube Hollow Polyhedron for Efficient Overall Water Splitting. *Journal of the American Chemical Society* **2018,** *140* (7), 2610-2618.
[16]Gopi, S.; Al-Mohaimeed, A. M.; Al-onazi, W. A.; Soliman Elshikh, M.; Yun, K., Metal organic framework-derived Ni-Cu bimetallic electrocatalyst for efficient oxygen evolution reaction. *Journal of King Saud University - Science* **2021,** *33* (3), 127352.
[17]Guo, Y.; Tang, J.; Wang, Z.; Kang, Y.-M.; Bando, Y.; Yamauchi, Y., Elaborately assembled core-shell structured metal sulfides as a bifunctional catalyst for highly efficient electrochemical overall water splitting. *Nano Energy* **2018,** *47*, 494-502.
[18]Lai, Y.; Xiao, L.; Tao, Y.; Gao, Z.; Zhang, L.; Su, X.; Dai, Y., Enhancing One-Dimensional Charge Transport in Metal-organic Framework Hexagonal Nanorods for Electrocatalytic Oxygen Evolution. *ChemSusChem* **2021,** *14* (8), 1830-1834.
[19]Wei, Y. S.; Sun, L.; Wang, M.; Hong, J.; Zou, L.; Liu, H.; Wang, Y.; Zhang, M.; Liu, Z.; Li, Y.; Horike, S.; Suenaga, K.; Xu, Q., Fabricating Dual-Atom Iron Catalysts for Efficient Oxygen Evolution Reaction: A Heteroatom Modulator Approach. *Angew Chem Int Ed Engl* **2020,** *59* (37), 16013-16022.
[20]Li, X.; Ma, D. D.; Cao, C.; Zou, R.; Xu, Q.; Wu, X. T.; Zhu, Q. L., Inlaying Ultrathin Bimetallic MOF Nanosheets into 3D Ordered Macroporous Hydroxide for Superior Electrocatalytic Oxygen Evolution. *Small* **2019,** *15* (35), 1902218.
[21]Diao, J.; Qiu, Y.; Liu, S.; Wang, W.; Chen, K.; Li, H.; Yuan, W.; Qu, Y.; Guo, X., Interfacial Engineering of W_2N/WC Heterostructures Derived from Solid-State Synthesis: A Highly Efficient Trifunctional Electrocatalyst for ORR, OER, and HER. *Adv Mater* **2020,** *32* (7), e1905679.
[22]Lu, K.; Gu, T.; Zhang, L.; Wu, Z.; Wang, R.; Li, X., POM-assisted coating of MOF-derived Mo-doped Co_3O_4 nanoparticles on carbon nanotubes for upgrading oxygen evolution reaction. *Chemical Engineering Journal* **2021,** *408*, 127352.
[23]Wang, C.; Shang, H.; Wang, Y.; Li, J.; Guo, S.; Guo, J.; Du, Y., A general MOF-intermediated synthesis of hollow CoFe-based trimetallic phosphides composed of ultrathin nanosheets for boosting water oxidation electrocatalysis. *Nanoscale* **2021,** *13* (15), 7279-7284.
[24]Hu, C.; Jin, H.; Liu, B.; Liang, L.; Wang, Z.; Chen, D.; He, D.; Mu, S., Propagating Fe-N_4 active sites with Vitamin C to efficiently drive oxygen electrocatalysis. *Nano Energy* **2021,** *82*, 105714.
[25]Li, J.; Liu, P.; Mao, J.; Yan, J.; Song, W., Structural and electronic modulation of conductive MOFs for efficient oxygen evolution reaction electrocatalysis. *Journal of Materials Chemistry A* **2021,** *9* (18), 11248-11254.
[26]Zhang, S. L.; Guan, B. Y.; Lu, X. F.; Xi, S.; Du, Y.; Lou, X. W. D., Metal Atom-Doped Co_3O_4 Hierarchical Nanoplates for Electrocatalytic Oxygen Evolution. *Advanced Materials* **2020,** *32* (31), e2002235.

[27]Chen, W.; Wang, C.; Su, S.; Wang, H.; Cai, D., Synthesis of ZIF-9(III)/Co LDH layered composite from ZIF-9(I) based on controllable phase transition for enhanced electrocatalytic oxygen evolution reaction. *Chemical Engineering Journal* **2021,** *414*, 128784.

[28]Liu, H.; Guan, J.; Yang, S.; Yu, Y.; Shao, R.; Zhang, Z.; Dou, M.; Wang, F.; Xu, Q., Metal-Organic Framework-Derived Co_2P Nanoparticle/Multi-Doped Porous Carbon as a Trifunctional Electrocatalyst. *Advanced Materials* **2020**, e2003649.

[29]Bagchi, D.; Phukan, N.; Sarkar, S.; Das, R.; Ray, B.; Bellare, P.; Ravishankar, N.; Peter, S. C., Ultralow non-noble metal loaded MOF derived bi-functional electrocatalysts for the oxygen evolution and reduction reactions. *Journal of Materials Chemistry A* **2021,** *9* (14), 9319-9326.

[30]Wang, X. T.; Ouyang, T.; Wang, L.; Zhong, J. H.; Ma, T.; Liu, Z. Q., Redox-Inert $Fe^{(3+)}$ Ions in Octahedral Sites of Co-Fe Spinel Oxides with Enhanced Oxygen Catalytic Activity for Rechargeable Zinc-Air Batteries. *Angewandte Chemie. International Ed. In English* **2019,** *58* (38), 13291-13296.

[31]Liu, C.; Wang, J.; Wan, J.; Cheng, Y.; Huang, R.; Zhang, C.; Hu, W.; Wei, G.; Yu, C., Amorphous Metal-Organic Framework-Dominated Nanocomposites with Both Compositional and Structural Heterogeneity for Oxygen Evolution. *Angewandte Chemie. International Ed. In English* **2020,** *59* (9), 3630-3637.

[32]Yang, S.; Chen, G.; Ricciardulli, A. G.; Zhang, P.; Zhang, Z.; Shi, H.; Ma, J.; Zhang, J.; Blom, P. W. M.; Feng, X., Topochemical Synthesis of Two-Dimensional Transition-Metal Phosphides Using Phosphorene Templates. *Angew Chem Int Ed Engl* **2020,** *59* (1), 465-470.

[33]Lu, Z.; Wang, K.; Cao, Y.; Li, Y.; Jia, D., Amino-functionalized iron-based MOFs modified with 2D FeCo(OH) hybrids for boosting oxygen evolution. *Journal of Alloys and Compounds* **2021,** *871*, 159580.

[34]Hou, J. G.; Zhang, B.; Li, Z. W.; Cao, S. Y.; Sun, Y. Q.; Wu, Y. Z.; Gao, Z. M.; Sun, L. C., Vertically Aligned Oxygenated-CoS_2–MoS_2 Heteronanosheet Architecture from Polyoxometalate for Efficient and Stable Overall Water Splitting. *Acs Catalysis* **2018,** *8* (5), 4612-4621.

[35]Li, Y.; Gao, Z.; Bao, H.; Zhang, B.; Wu, C.; Huang, C.; Zhang, Z.; Xie, Y.; Wang, H., Amorphous nickel-cobalt bimetal-organic framework nanosheets with crystalline motifs enable efficient oxygen evolution reaction: Ligands hybridization engineering. *Journal of Energy Chemistry* **2021,** *53*, 251-259.